Construction and Building Materials 400 (2023) 132748

Contents lists available at ScienceDirect

Construction and Building Materials

journal homepage: www.elsevier.com/locate/conbuildmat

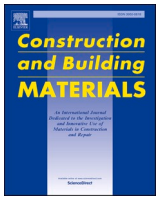

Surface treatment of inorganic modifier for improving carbonation resistance of geopolymers

Xuezhong LI, Zhuguo LI *

Graduate School of Science and Technology for Innovation, Yamaguchi University, 2-16-1, Tokiwadai, Ube, Yamaguchi 755-8611, Japan

ARTICLE INFO

Keywords:
Geopolymer
Carbonation resistance
Sodium aluminate
Surface modifier
Fly ash
Blast furnace slag
Neutralization

ABSTRACT

Geopolymer (GP) is a low-carbon binder with the potential to replace Portland cement in reinforced concrete, however, the risk of corrosion to reinforced steel bars due to its low carbonation resistance must be addressed. This study proposed the use of an inorganic surface modifier, sodium aluminate solution (AN), to improve the carbonation resistance of GP. The effects of AN surface treatment on carbonation depths were investigated for GP mortars using fly ash (FA), ground granulated blast furnace slag (BFS), or their blend as active fillers. Rational AN surface treatment conditions and microstructural changes of treated GPs were also discussed. The obtained results show that AN surface treatment can significantly reduce carbonation rates of FA/BFS blend-based GP, and largely delay the onset of neutralization of heat-cured GP through the reduction of cracks and the formation of Na-gmelinite and gismondine, which refine the surface layer of GP. The surface modification using 40 wt%-AN solution reduced carbonation rate coefficient by about 70% for the FA/BFS blend-based GP cured at 80 ℃, and by above 30% for that cured at 20℃. The larger the FA blending ratio or the smaller the liquid-active filler ratio, the greater the improvement in carbonation resistance of FA/BFS blend-based GPs, caused by the AN surface modification. For the ambient-cured GP, repeated surface treatment is preferred, while for the heat-cured GP, once treatment is enough, and seal curing after the AN surface treatment is recommended regardless of the curing method.

1. Introduction

Many industrial wastes, such as fly ash (FA) from coal-fired power plants, blast furnace slag, and municipal solid waste incineration ash, etc., are released to pose challenges in environmental problems. Geopolymer (GP) is a type of inorganic polymer that is possibly made from these wastes as precursors [1]. Moreover, if used as cementitious materials, GP can potentially lower the carbon footprint of the cement industry [2,3]. It has attracted considerable attention also because of its good early strength development, ductility, bonding strength with reinforced bar, chemical corrosion resistance, and fire resistance [4–11]. Thus, GP is a promising candidate as an alternative to Portland cement (PC) for the construction industry.

Typical geopolymer using metakaolin or fly ash has a three-dimensional structure formed by aluminosilicate minerals [12]. Compared to PC, FA-based geopolymer can reduce about 60% of CO_2 emission [13], but it needs heat-curing. Ground granulated blast furnace slag (BFS) is usually added in FA-based geopolymer to raise its strength, even cured at room temperature[14]. Thus, recently FA and BFS are usually used together as precursors of GP. Although there are many kinds of research on GPs made from different precursors, including but not limited to FA, BFS and metakaolin, most of them have focused on mechanical properties, acid/fire resistance, reaction products and microstructure [15–21].

Steel bars are often used with concrete in engineering. To reduce the corrosion risk of steel bars in reinforced concrete, PC concrete should be kept to have certain alkalinity, generally pHgreater than11.5. Since carbonation would lower the alkalinity of concrete, high carbonation resistance of concrete is required to ensure the durability of reinforced concrete structures. However, compared to PC concrete, the carbonation resistance of geopolymer materials is lower [22–25]. Pouhet R., et al. [26] found a very fast decrease in the pH of pore solution in metakaolin-based geopolymer and almost total carbonation under natural conditions after only 14 days. For the same compressive strength (25.0~29.0 MPa) of concrete, the carbonation rate coefficient (a) of 70% FA/30% BFS blend-based GP concrete cured in the ambient air is two times higher than that of PC concrete [27]. Curing at ambient temperature yields a lower carbonation resistance compared to heat-curing, and the

* Corresponding author.
E-mail address: li@yamaguchi-u.ac.jp (Z. LI).

https://doi.org/10.1016/j.conbuildmat.2023.132748
Received 7 May 2023; Received in revised form 30 July 2023; Accepted 31 July 2023
Available online 3 August 2023

FA/BFS blend-based GP concrete cured in the ambient air has a faster carbonation rate than the PC concrete in the early age of accelerated carbonation test [24]. The volcanic pozzolan/BFS blend-based geopolymers showed good carbonation resistance in some formulations [28], but the carbonation resistance are still dependent on the BFS, and the reactivity and fineness of pozzolan, etc. [29]. For the practical use of GP in reinforced concrete, it is essential to develop methods to reduce the carbonation rate of GP [30,31].

Two reasons are generally considered to cause the low resistance of geopolymer to carbonation. Firstly, the polymerisation reaction of geopolymer is a dehydration reaction. The channels, pores and cracks may be generated in hardened GP due to moisture escape and dry shrinkage, which cause CO_2 to diffuse inside easily. FA/BFS blend-based GP concrete cured in the ambient air has large dry shrinkage [32]. The second is that the residual sodium or potassium in the pores of GP, which brings alkalinity to GP, is more soluble than $Ca(OH)_2$ in PC concrete and thus easily reacts with CO_2. Moreover, the generated sodium carbonate or potassium carbonate is alkaline, but since they are water soluble, they leach out easily from GP concrete during repeated drying and wetting or in a moisture environment, causing the concrete to neutralize [33]. These two reasons also make it difficult to improve the neutralization resistance of GP by mixture design.

Susan A., et al. [34] investigated the carbonation resistances of three silicate-activated slags (AAS) to develop a method to improve the carbonation resistance of GP by adding MgO, and found that with higher MgO content (>5%), the hydrotalcite is formed in addition to C–A–S–H gels, which takes up CO_2 and thus retards the carbonation of GP. But the degree of improvement is limited, and no other research literature was found to confirm this improvement. Pasupathy et al. [25] reported that the GP concrete, only using NaOH or KOH solution as alkali activator, has a relatively greater carbonation resistance than that using a blend of NaOH or KOH and sodium silicate. But, the carbonation resistance of NaOH or KOH activated GP concrete is not yet enough for practical application.

Portland cement, used in PC concrete as the binder, has stable components and properties, so the carbonation resistance of PC concrete can be simply improved by reducing the water-cement ratio. However, there are many types of active fillers and alkali activators used in geopolymers, and the GP formulations are diverse. Reducing the liquid-filler ratio may make geopolymer dense, but, as the aforementioned reasons of low carbonation (or neutralization) resistance of GP, the carbonation resistance of GP is greatly dependent on its initial alkalinity of residual alkali activator, and the environment where it is located. Thus, it is worth considering the surface treatment besides careful mixture design of GP materials.

Zhang et al. [35] found that the organic coating of waterborne epoxy resin functions well in shrinkage reduction, anti-abrasion, and anti-chloride ion diffusion of marine GP concrete, but has no improvement in carbonation resistance. Kitasato & Li et al. [36] confirmed the organic coating agent composed of hydrocarbon esters/silane compounds can greatly improve the carbonation resistance of GP. However, the durability and water resistance of the organic coating layer are obviously issues.

Silicate solution is often used as a surface modifier for PC concrete, based on the reaction between silicate ions and hydrate of PC (calcium hydroxide) to form the calcium silicate that makes the surface layer of PC concrete dense [37,38]. Moreover, in the case of using lithium silicate, residual lithium silicate will solidify to fill pores in concrete [39], which also refines the PC concrete. The method and principle of surface modification of PC concrete undoubtedly shows the feasibility and gives a reference in developing inorganic surface modifier for GP materials.

Considering there are almost few effective proportioning methods to improve the carbonation resistance of GP materials, and because organic surface modifiers are not durable, an inorganic surface modifier: aqueous sodium aluminate solution (AN) was proposed for GP materials in this study. We compared the carbonation depths of FA or/and BFS-based GP mortars with and without surface modification of AN by the accelerated carbonation test to confirm if the AN surface treatment can improve the carbonation resistance of GP materials. Then, the factors influencing the AN surface treatment effect were discussed in detail, including mix proportions of GP, curing method, and surface treatment conditions. Finally, we investigated the air permeability and the chemical and microstructural changes of the GPs after the AN surface treatment to clarify the mechanisms of carbonation resistance improvement. This study contributed to the development of effective and durable surface modification techniques for GP materials, and opens new possibilities for enhancing the performance of GP in various applications.

2. Experimental program

2.1. Raw materials used

The fly ash (FA) of JIS (Japanese Industrial Standards) grade II and the ground granulated blast furnace slag (BFS) of JIS 4000 class were used as active fillers (AF) of GP mortars, which physical properties and chemical compositions are shown in Tables 1 and 2, respectively. The metal oxide contents and density of sodium aluminate solution (AN) with a concentration of 40 wt% are presented in Table 1, too. Other AN solutions with different concentrations were prepared by diluting 40 wt % AN solution with distilled water. Sea sand, washed in advance with tap water, was used as fine aggregate of the GP mortars.

Three kinds of alkali activator solution (AS), named AS01, AS11 and AS31, were used, which were sodium hydroxide solution (NH) with 10 mol or a mixture of water glass aqueous solution (WG) and the NH according to the volume ratio of WG: NH = 1:1 or 3:1, as shown in Table 3. The WG was prepared by diluting JIS No.1 grade sodium silicate (Na_2SiO_3) with distilled water by a volume ratio of 1:1.

2.2. Mix proportions of GP mortars

The mix proportions of GP mortars used in this study are shown in Table 4. Based on the preliminary investigation, we found that series No.1 had adequate fluidity for specimen production, thus, it was used as the control mixture. Then, the other GP mortars were designed by adjusting the BFS blending ratio, WG/NH ratio by volume, and liquid-fillers ratio by mass, as shown in Table 4, on the basis of series No.1. In this experiment, the ratio of fine aggregates (S) to AF was 2.0 throughout by mass.

Also, for clarifying appropriate AN treatment conditions, the effects of the AN solution concentration, AN surface treatment frequency within 3 days, the age of mortar specimen when the AN surface treatment, whether the mortar specimens were sealed after the AN surface treatment during curing, and curing temperatures were investigated, as summarised Table 5. The GP specimens with the same mix proportion were tested and the effects of different conditions of AN treatment were reflected on the carbonation degree of GP mortars.

2.3. Specimen preparation

The experimental process is shown in Fig. 1. A Hobart planetary mortar mixer was used to mix the GP mortars. The active fillers and sea

Table 1
Physical properties of raw materials used.

Raw material	Properties, etc.
FA	Specific gravity: 2.30, Blaine fineness: 4392 cm^2/g
BFS	Specific gravity: 2.88, Blaine fineness: 4180 cm^2/g
Sea sand	Oven-dry density: 2.51, surface-dry density: 2.56, specific water absorption: 1.81%, solid content: 66.7%, F.M. 2.87
Sodium aluminate solution	Compositions: Na_2O 19%, Al_2O_3 20%, Molar ratio (Na_2O/Al_2O_3): 1.56, Specific gravity: 1.49 (40 wt% concentration)

Table 2
Chemical compositions of FA and BFS (XRF analysis).

Active filler	Chemical compositions (%)								
	SiO_2	Al_2O_3	CaO	Fe_2O_3	MgO	Na_2O	K_2O	TiO_2	others
FA	59.10	23.91	3.48	7.37	1.06	1.07	1.68	1.27	1.06
BFS	34.67	14.46	43.13	0.34	5.50	0.25	0.25	0.55	0.85

Table 3
Alkali activator solution's components and density.

Alkali activator solution	WG: NH, by volume	Specific gravity	Mole ratio of SiO_2/Na_2O	Molarity of Na_2O (mole/L)
AS01	0:1	1.330	0	5.000
AS11	1:1	1.359	0.696	2.438
AS31	3:1	1.374	1.255	3.108

Table 4
Mix proportions of GP mortars.

Series No.	Parameters	WG: NH (WG/AS)	AS/AF	BFS: FA (BFS/AF)	S/AF
1	Control mix	3:1 (0.75)	0.5	3:7(0.3)	2.0
2	BFS blending			0:1 (0)	
3	ratio			1:1 (0.5)	
4				1:0 (1)	
5	WG/NH ratio	0:1 (0)		3:7 (0.3)	
6		1:1 (0.5)			
7	AS/AF	0.75	0.45		
8			0.55		

Note: 25 wt.% AN solution was applied twice at 3 days old, and the specimens were sealed as cured till 28 days after the treatment.

Table 5
Conditions of AN surface treatment.

Series No.	Factors	Mortar Age, frequency of AN application	AN concentration by mass (%)	State during curing
9	Control	No-AN application		Sealed
10	Age when the AN	7 days, twice	25	
11	was applied	20 days, twice		
12	Concentrations of	3 days, twice	10	
13	AN		20	
14			30	
15			40	
16	AN treatment frequency	3 days, once	25	
17	Sealing state during curing	3 days, twice		Not sealed

Note: Mix proportions of GP mortar of series 9–17 were the same as those of series No.1 shown in Table 4.

sand were first put into the mixer and mixed for 1 min. Then, the alkali activator was added and mixed for 2 min. to get GP mortar. Finally, freshly mixed GP mortar was used to produce the prism specimens with a 4 cm side length of square section and 16 cm length, which were used for the accelerated carbonation test. Each of the mortar specimens was compacted by a table vibrator for 1 min, followed by levelling the top surface with a metal spatula. After being sealed with water-retention tape, half of the specimens were cured in the air at 20 ℃ and R.H. 60% for 28 days (hereafter referred to as 20 ℃ curing), and another half were first cured in the air at 80 ℃ for 8 h, then stored in a 20 ℃ environmental chamber till 28-day age (hereafter referred to as 80 ℃ curing). The temperature and time conditions set for the two curing methods are commonly used in the field of geopolymer research. The specimens were demoulded at 1 day age. The six surfaces of half of the prismatic specimens were applied with AN solution at the ages of 3, 7 and 28 days, respectively, according to the treatment conditions shown in Tables 4, 5. Although the application was conducted by a brush according to the number of AN application determined in advance, the amount of AN solution applied was uncertain, depending on the surface conditions of specimen such as denseness and moisture content. Fig. 2 shows the appearance of 80 ℃-cured GP mortars before and after AN surface treatment. After AN treatment, surfaces of GP mortar becomes slightly white.

2.4. Property test, chemical and microstructure analysis

(1) Accelerated carbonation test

After 28 days of curing, four surfaces (two ends, top and bottom surfaces) of mortar specimens were sealed with an airtight sealing tape to ensure that CO_2 diffuses into the specimens only through the two side surfaces. Then, the specimens were placed into a carbonation test chamber with 5% of CO_2 concentration, 20 ℃, and R.H. 60%. At an interval of two weeks, the mortar specimen was cut at about 10 mm interval to measure carbonation depth. It should be noted that during the cutting, to ensure that the alkali matters were not washed away, spraying water was not used as a dust countermeasure.

The depth of the colourless region from the surface of the prism specimen was measured at 3 min. strictly after spraying the 1% phenolphthalein solution. The average value of six depths, three values on one side and 1 cm interval respectively, was recorded as carbonation depth. After the measurement of carbonation depth, the cut sections were sealed with airtight tape, and the remained GP mortar samples were returned to the CO_2 chamber to continue the carbonation test. The accelerated carbonation test lasted 18 weeks.

(2) Air permeability measurement

The air permeability of series No. 1 with and without the AN surface treatment was evaluated according to NDIS 3436–2 by a digital air permeability tester at 28-day age. The plate specimens with 160 mm length, 120 mm width and 40 mm thickness were prepared and used, which were cured by the 20 ℃-curing method and the 80 ℃-curing method, respectively. The air permeabilities of specimens with and without AN treatment were tested to compare the effect of AN on the air permeability of GP mortars.

(3) Strength measurement

For clarifying the effect of the AN-surface treatment on the strength of BFS/FA blend-based GP, we measured the flexural and compressive strengths of mortars of series No.1 and No.3, with and without the AN treatment, using a universal testing machine on 28-day age. The specimens were prisms with dimensions of 40 mm×40 mm×160 mm, which were cured by the 80 ℃-curing method or the 20 ℃-curing method. The flexural strength was an average of three prismatic specimens for each mixture, while the compressive strength was an average of six fractured prismatic pieces after the flexural test.

(4) SEM-EDS and XRD analysis

To investigate the microstructural change and reaction products of

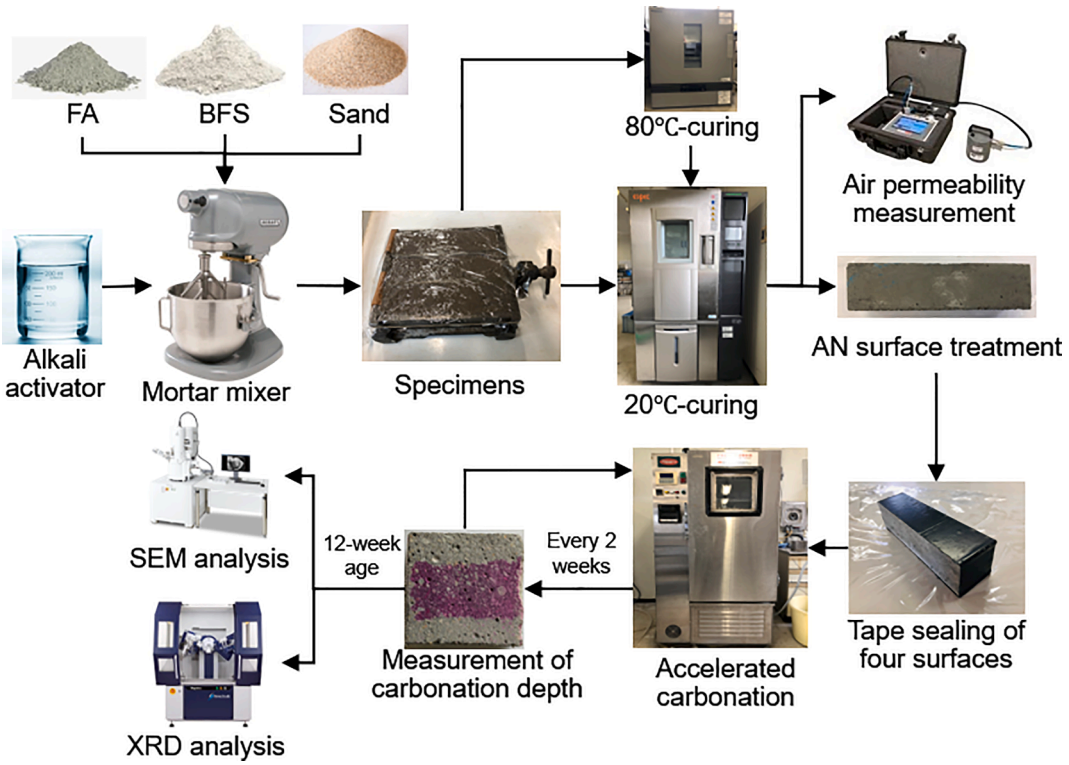

Fig. 1. Experimental process.

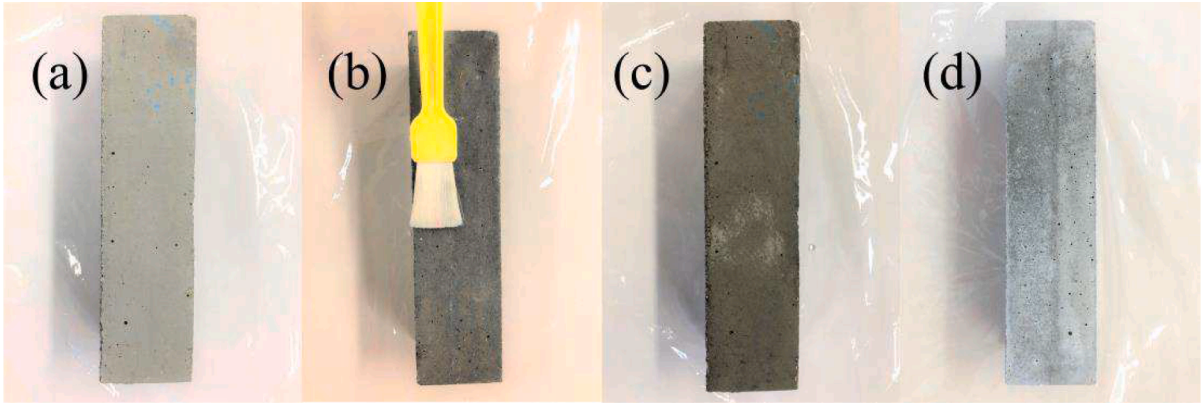

Fig. 2. The surfaces of geopolymer mortar specimens (40 × 40 × 160 mm): (a) before treatment, (b) AN surface treatment by brush, (c) right after AN treatment, and (d) AN-treated specimen at 28-day age.

surface-modified GPs, XRD (X-ray diffraction) and SEM-EDS (scanning electron microscopy) analyses of GP mortars with and without AN surface treatment at 3-day age were conducted. The specimens analysed were sampled from GP mortars which were FA-based (series No. 2), BFS-based (series No. 4), and FA/BFS-based (series No. 1), respectively, which were cured at 80 ℃ for 8 h and then 20 ℃ for 27 days.

After the accelerated carbonation test of 12 weeks, the used samples for the SEM-EDS and XRD analyses were collected from the surface layer with 1 mm depth, where it was believed that the AN solution diffused from colour change. The samples of the SEM-EDS analysis were pre-treated by embedding in resin and then polishing. The SEM-EDS analysis was taken under 15 kV accelerating voltage. ZAF (atomic number, absorption, and fluorescence) corrections were automatically done for point analysis data. The XRD analysis used a CuKα source, 40 kV-120 mA power supply, 1° -1° -1°-0.3 mm slit method, scanning speed 4°/min, and 0.02° step scans in the 2θ range of 5-60°.

3. Test results and discussion

3.1. The effects of mix proportions on the effectiveness of AN surface treatment

The diffusion of carbon dioxide and the carbonation are greatly influenced by the features of matrix mortar such as denseness and chemical compositions[24], and the presence of coarse aggregate greatly affects the measurement accuracy of carbonation depth because coarse aggregate particles make the front line of carbonation into a jagged curve. Thus, in this study, we used GP mortars instead of concrete to discuss the effect of AN surface treatment on the carbonation resistance of GP materials.

The effects of AN treatment on the carbonation resistance of GP mortar with different mix proportions and with the different treatment conditions were discussed on the basis of regression analysis of carbonation depth - carbonation time relationship for different mortars

and treatment conditions. As described later, due to the AN surface treatment, the carbonation depth of part of the specimens could be detected only after a period, so we used Eq. (1) for the regression analysis.

$$C_d = a \cdot \sqrt{CO_2\%/5.0} \cdot \sqrt{t - b} \quad (1)$$

where C_d is carbonation depth (mm), t is carbonation period (week), CO_2% represents CO_2 concentration (%), a is proportional coefficient (mm/$\sqrt{}$week), and b is elapsed time until the depth of carbonation can be detected, i.e., onset time of neutralization (week, ≧0).

In Eq. (1), the proportional coefficient a implies the rate of increase of the carbonation depth with elapsed time and therefore is called carbonation rate coefficient. The smaller the a, the higher the carbonation resistance of GP mortar. And the larger the b, the later the onset of neutralization, and therefore the higher the initial carbonation resistance.

(1) Effect of FA/BFS ratio

Fig. 3 (a) and (b) show the test results of the relationship between the carbonation depth and the elapsed time for the GP mortars with different FA/BFS blending ratios by mass. Compared to the 20 ℃-cured mortars, in case of the 80 ℃-cured BFS/FA blend-based mortars had smaller carbonation depths for the same elapsed time. This is because heat-curing promotes the reaction of FA and BFS, especially FA, with more products leading to a denser microstructure at 28-day age [40,41]. However, the carbonation resistance of the BFS sole-based GP mortar cured by the heating method was lower compared with the BFS sole-based GP mortar cured in the ambient air. This is because the dry shrinkage and moisture escape arising from the heat-curing resulted in more porosity and larger cracks in the BFS-based GP mortar [42,43]. FA-based GP mortar without BFS addition was easy to carbonate, the carbonation reached the centre of the 80 ℃-cured prism specimen with 40 mm side length at two weeks, but the AN surface treatment delayed the complete carbonation time from two weeks to one month. On the other hand, the BFS-based GP mortar cured in the ambient air had no detectable carbonation depth within 18 weeks, regardless of the AN surface treatment, and thus the benefit of the AN surface treatment was not confirmed. This is because the reaction products are few in the FA sole-based GP, which leads to a high porosity of GP [44].

As shown in Fig. 3 (a), For part of the 80 ℃-cured mortar specimens with AN surface treatment, the time to detect the depth of carbonation was delayed by 2–4 weeks. Therefore, we used the two parameters a, b in Eq. 3 to characterize the carbonation resistance of the surface-treated GPs, of which b represents delayed time, and a is the carbonation rate coefficient as usual. The regression equations for the relationship between carbonation depth and time, and the obtained a, b values are shown under each graph.

The smaller the a-value or the larger the b-value, the higher the carbonation resistance. It is indicated from the a, b-values and the decrease of a-value shown in the tables of Fig. 3 that the heat-cured GP mortars had higher carbonation resistance than those with ambient-curing, and that the AN surface treatment was more effective for the heat-cured GP mortars. However, regardless of the curing method, the AN surface treatment had an obvious effect on the carbonation resistance improvement. That is, due to the surface treatment, the a value was decreased or/and the b value is larger than zero.

It is obvious from Fig. 3 that the lower the blending ratio of BFS, the larger the carbonation rate coefficient of the non AN-treated mortar. However, the mortar with a larger carbonation rate coefficient attained a better improvement from the viewpoint of the decrease of a value. In the case of 30% of the BFS blending ratio, the AN treatment yielded the highest decrease in the carbonation rate coefficient a. Therefore, it is concluded that the AN surface modifier is more suitable for BFS/FA blend-based GP with a low BFS blending ratio. Considering that the

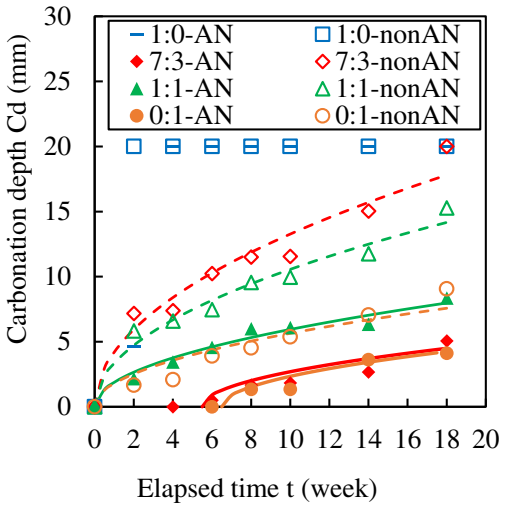

FA/BFS	AN treatment	Non-AN treatment	Decrease of a (%)	b (week)
1:0	-	-	-	-
7:3	$C_d = 1.27\sqrt{t\text{-}5.5}$ R² = 0.876	$C_d = 4.19\sqrt{t}$ R² = 0.990	69.73	5.5
1:1	$C_d = 1.88\sqrt{t}$ R² = 0.993	$C_d = 3.33\sqrt{t}$ R² = 0.994	43.54	0
0:1	$C_d = 1.25\sqrt{t\text{-}7}$ R² = 0.934	$C_d = 1.78\sqrt{t}$ R² = 0.971	29.77	7

(a) 80 °C-curing

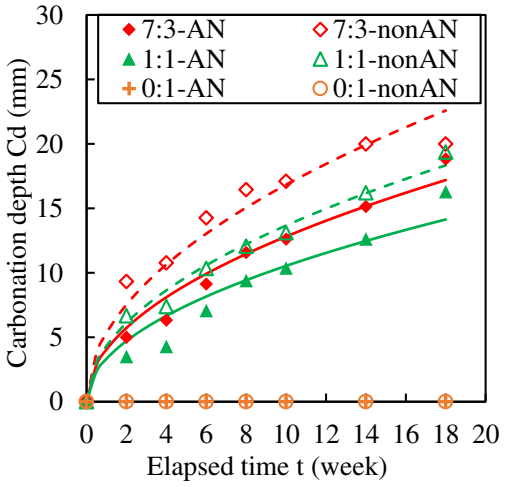

FA/BFS	AN treatment	Non-AN treatment	Decrease of a (%)	b (week)
7:3	$C_d = 4.05\sqrt{t}$ R² = 0.932	$C_d = 5.32\sqrt{t}$ R² = 0.924	23.87	0
1:1	$C_d = 3.33\sqrt{t}$ R² = 0.981	$C_d = 4.32\sqrt{t}$ R² = 0.997	22.89	0
0:1	-	-	-	-

(b) 20 °C-curing

Fig. 3. Carbonation depth of GP mortars with different FA/BFS ratios (Series No. 1, 2, 3, 4).

carbonation resistance is mainly dependent on the porosity of GP [25,45], a smaller BFS blending ratio leads to large porosity and large pore size [46,47], which makes the AN solution penetration easier and thus brings better modification. For the 20 ℃-cured GP mortars, although the carbonation rate coefficient was reduced due to the AN surface treatment, the decrease degree was smaller compared to the 80 ℃-cured mortar with the same FA/BFS blending ratio, and the beginning time of carbonation was not delayed. Drying shrinkage cracks caused by heat-curing promote internal penetration of the AN solution is guessed to be the cause of this phenomenon.

(2) Effect of WG/NH ratio

Fig. 4 (a) and (b) show the relationship between the carbonation depth and the elapsed time for the 30% BFS/70% FA blend-based GP mortars produced by different AS solutions and cured by the 20 ℃ method or the 80 ℃ method. The AN surface treatment yielded a significant enhancement in carbonation resistance for GP mortars, regardless of the curing method. Furthermore, even though the AS solution used in GP mortar was changed, the AN surface treatment was still more effective for the 80 ℃-cured specimens in reducing the *a* value and increasing the *b* value, i.e. the improvement of carbonation resistance was greater for the 80 ℃-cured GPs. When treated with the AN solution, the 80 ℃-cured GP mortar with a WG/NH volumetric ratio of 1:1 was not carbonated during the accelerated carbonation period of 18 weeks. The continuous dissolution of silicate from the precursors due to the activation of alkali forms many free Si-O-Si tetrahedral monomers, which contribute to the SiO4 and AlO4 linking. The increase of SiO2/Na2O mole ratio is reported to promote the formation of N-A-S-H gels in GPs [48]. However, the apparent porosity of GP would increase when the mole ratio of SiO2/Na2O exceeds 0.806 [49]. This can explain why the carbonation depths of the GP mortar specimens with a WG/NH ratio of 3:1 (SiO2/Na2O = 1.25) were greater than those with a WG/NH ratio of 1:1 (SiO2/Na2O = 0.69). More residual Na+ present in pores is another reason why the GP mortar specimens with a WG/NH ratio of 1:1 had smaller carbonation depths. That is, an appropriate SiO2/Na2O molar ratio is essential to achieve high carbonation resistance of GP. We found that in the case of 80 ℃-curing, the specimen with WG/NH=0:1 had a lower improvement degree of carbonation resistance than the specimen with WG/NH=3:1, while the trend was opposite in the case of 20 ℃-curing. At present we are not clear about the reasons. The AN surface treatment effectiveness is estimated to be influenced by a combination of factors such as drying shrinkage cracks, residual Si^{4+}, Na^{+} content, and the porosity of GP.

(3) AS/AF ratio

Fig. 5 (a) and (b) show the experimental results of the relationship between the carbonation depths and the elapsed time for the 30% BFS/70% FA blend-based GP mortars with different liquid-active filler (AS/AF) ratios. Regardless of curing method, the smaller the AS/AF ratio, the smaller carbonation depth for the same elapsed time. As reported in other studies, a lower AS/AF ratio leads to finer pores and lower porosity [50], less drying shrinkage [51], and thus contributes to a higher carbonation resistance of GP materials [24,52].

It is clearly observed that the surface treatment of AN solution improved the carbonation resistance of the GP mortars from Fig. 5, though the 80 ℃-cured GP mortars got a much reduction in the carbonation depth than the 20 ℃-cured specimens. And the AN surface treatment greatly delays the beginning time of carbonation of the 80 ℃-cured GP mortars, as shown in Fig. 5, thus the *b* value is 4~8 weeks. That is to say, in the general range of AS/AF ratio, regardless of AS/AF ratio, the carbonation resistance of BFS/FA blend-based GP can be expected to be improved by the AN surface treatment. In the case of heat-curing, the decrease of *a* value can be reduced by more than 70%. And it can be concluded that the smaller the AS/AF ratio, the higher the

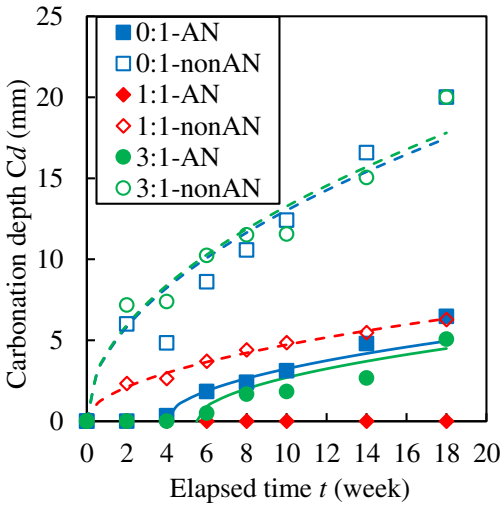

WG /NH	SiO_2 /Na_2O	AN treatment	Non-AN treatment	Decrease of *a* (%)
0:1	0.00	$C_d = 1.32\sqrt{t-4}$ $R^2 = 0.918$	$C_d = 4.11\sqrt{t}$ $R^2 = 0.978$	67.86
1:1	0.69	b>18	$C_d = 1.49\sqrt{t}$ $R^2 = 0.998$	-
3:1	1.25	$C_d = 1.27\sqrt{t-5.5}$ $R^2 = 0.876$	$C_d = 4.19\sqrt{t}$ $R^2 = 0.990$	69.68

(a) 80 ℃-curing

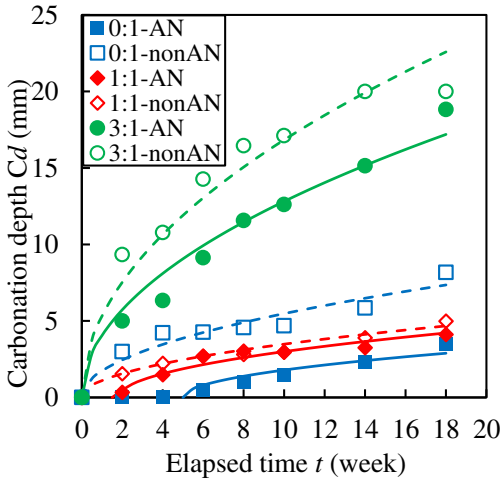

WG/ NH	SiO_2/ Na_2O	AN treatment	Non-AN treatment	Decrease of a (%)
0:1	0.00	$C_d = 0.80\sqrt{t-4}$ $R^2 = 0.909$	$C_d = 1.73\sqrt{t}$ $R^2 = 0.985$	53.74
1:1	0.69	$C_d = 1.04\sqrt{t-1.8}$ $R^2 = 0.882$	$C_d = 1.10\sqrt{t}$ $R^2 = 0.958$	4.96
3:1	1.25	$C_d = 4.05\sqrt{t}$ $R^2 = 0.993$	$C_d = 5.32\sqrt{t}$ $R^2 = 0.992$	23.87

(b) 20 ℃-curing

Fig. 4. Carbonation depth of GP mortars with different WG/NH ratios (Series No. 1, 5, 6).

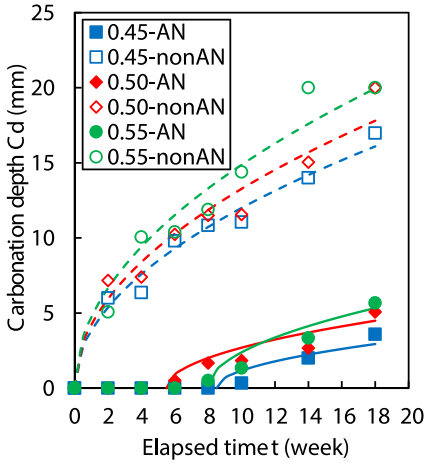

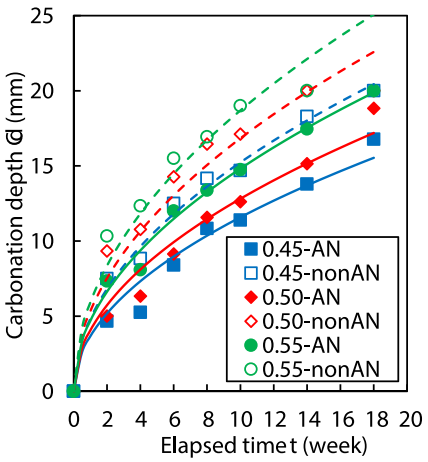

AS/AF	AN treatment	Non-AN treatment	Decrease of a (%)	b (week)
0.45	$C_d = 0.95\sqrt{t\text{-}8.5}$ $R^2 = 0.963$	$C_d = 3.79\sqrt{t}$ $R^2 = 0.995$	74.87	8.5
0.50	$C_d = 1.27\sqrt{t\text{-}5.5}$ $R^2 = 0.876$	$C_d = 4.19\sqrt{t}$ $R^2 = 0.990$	69.73	5.5
0.55	$C_d = 1.37\sqrt{t\text{-}8}$ $R^2 = 0.839$	$C_d = 4.70\sqrt{t}$ $R^2 = 0.991$	64.14	8

(a) 80 °C-curing

AS/AF	AN treatment	Non-AN treatment	Decrease of a (%)	b (week)
0.45	$C_d = 3.66\sqrt{t}$ $R^2 = 0.992$	$C_d = 4.81\sqrt{t}$ $R^2 = 0.998$	23.97	0
0.5	$C_d = 4.05\sqrt{t}$ $R^2 = 0.993$	$C_d = 5.32\sqrt{t}$ $R^2 = 0.992$	23.87	0
0.55	$C_d = 4.68\sqrt{t}$ $R^2 = 0.998$	$C_d = 5.91\sqrt{t}$ $R^2 = 0.993$	20.71	0

(b) 20 °C-curing

Fig. 5. Carbonation depth of GP mortars with different AS/AF ratios (Series No. 1, 7, 8).

improvement effectiveness from the decreasing degree of the *a* value. When the AS/AF ratio was 0.45, the starting point of carbonation was delayed to 8 weeks. However, the specimen with an AS/AF ratio of 0.55 had a longer delaying time of carbonation (*b* value) than the specimen with an AS/AF ratio of 0.50, which suggests that the *b* value depends on the AN's permeation ability, that is, the initial porosity of GP that is influenced by the AS/AF ratio. If the AN solution forms a dense layer in the surface layer of GP, this dense layer would delay the start of carbonation. The *b* value depends on the thickness and denseness of this dense layer, as shown in Fig. 6. Once the carbonation starts behind this dense layer, the rate of carbonation will depend on the degree of denseness and alkalinity inside the GP. The 20 ℃-cured mortar specimen had a relatively higher water content at 3-day age, compared to the 80 ℃-cured specimen. High water content reduces the AN's inside permeation ability, which correspondingly reduces the effectiveness of AN surface treatment.

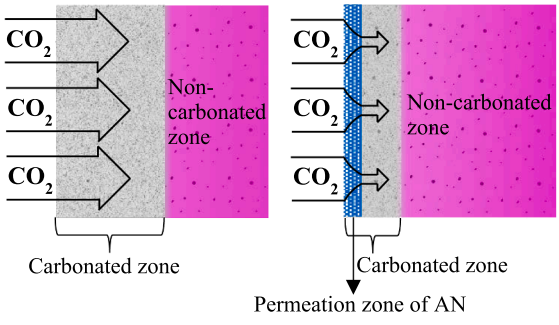

(a) Non-AN treatment (b) AN treatment

Fig. 6. Schematic representation of the carbonation of mortar.

3.2. *The effects of treatment conditions on the effectiveness of AN surface treatment*

(1) Time points of AN treatment

Fig. 7 presents the carbonation depths of the 70% FA/30% BFS blend-based GP mortars, which were cured in a sealed state and treated with the 25 wt% AN solution on the surfaces at different material ages. As shown in Fig. 7 (a), the AN surface treatment at 3-day age led to the maximum decreases in the carbonation depth of the 80 ℃-cured specimen, compared to the treatment at 7 days and 20 days, though the two later treatments also reduced the carbonation depth. On the other hand, according to the data distribution in Fig. 7 (b), for the 20 ℃-cured specimen, the AN surface treatment at 3-day age also greatly reduced the carbonation depth, while the treatment at 7-day and 20-day ages had almost no reduction effect. The reasons for these results are not entirely clear to us, but are discussed below.

Although the curing of the specimens was performed in a sealed state with plastic tape, the sealing with plastic tape or film does not strictly prevent the loss of moisture from the specimen. Thus, for the heat-cured specimens, after the 8-hour 80 ℃ curing, the water content should decrease greatly [51], benefiting the internal diffusion of the AN solution. It is reported that no matter whether sodium silicate or sodium hydroxide is used as an alkaline activator, the compressive strength reaches its ultimate strength at 7 days if heat-curing [53]. Accordingly, after 7 days, GP has considerable strength and denseness. Although the increase of denseness is favourable to carbonation resistance, it makes the internal diffusion of AN solution difficult. Therefore, the AN solution gained the best diffusion when the surface treatment was performed at 3 days, leading to the largest decrease of carbonation depth.

However, for the 20 ℃-cured specimens, since they were cured in a sealed state with plastic tape for 28 days, we believe that they had high moisture during the curing. The reaction products undoubtedly increased with age, i.e. the denseness of the specimen increased with age [44,54,55]. The high water content and the increase in denseness added difficulties to the internal diffusion of the AN solution. Therefore, the AN

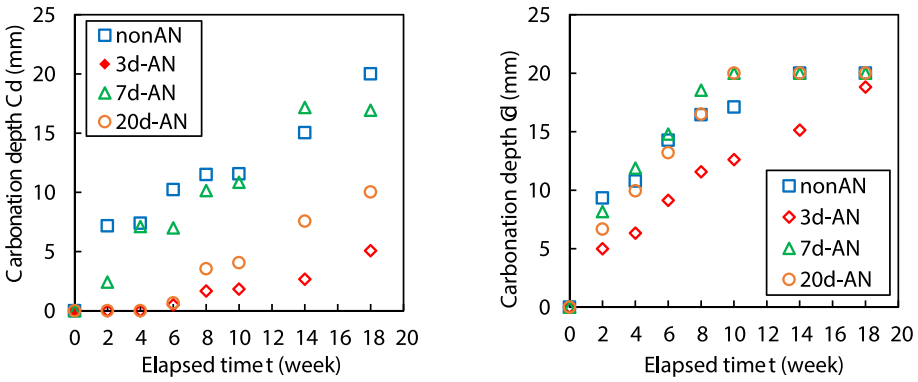

Fig. 7. Carbonation depth of GP mortars with AN treatment at different ages (Series No. 1, 9, 10, 11).

surface treatment at the 7 or 20-day age for the 20 ℃-cured specimens had almost no effect on the improvement of carbonation resistance. However, at the 3-day age, although the water content was high, the reaction products were few and the specimen is not yet dense, thus, the AN solution could have a certain degree of internal diffusion. Therefore, for the specimen sealed and cured at room temperature, a certain improvement effect was observed for the treatment at 3-day age.

We found that the AN surface treatment at the 20-day age was better

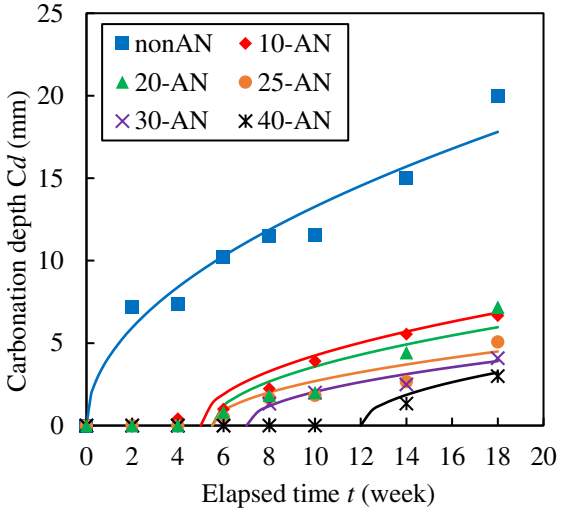

Conc. of AN	Regressive equation and R^2	Decrease of a (%)	Increase of b (week)
Non-AN	$C_d = 4.19\sqrt{t}$ $R^2 = 0.990$	-	-
10%	$C_d = 1.40\sqrt{t\text{-}5}$ $R^2 = 0.892$	54.75	3.5
20%	$C_d = 1.88\sqrt{t\text{-}5.5}$ $R^2 = 0.907$	59.81	5.5
25%	$C_d = 1.27\sqrt{t\text{-}5.5}$ $R^2 = 0.876$	69.73	5.5
30%	$C_d = 1.17\sqrt{t\text{-}7}$ $R^2 = 0.966$	71.91	7
40%	$C_d = 1.31\sqrt{t\text{-}12}$ $R^2 = 0.961$	68.68	12

(a) 80 ℃-curing

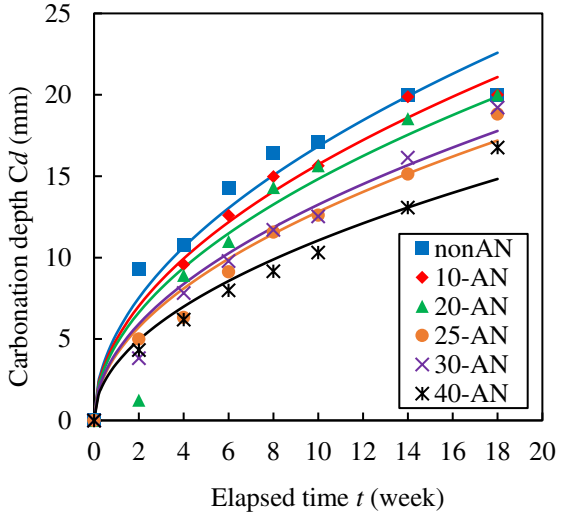

Conc. of AN	Regressive equation and R^2	Decrease of a (%)	Increase of b (week)
Non-AN	$C_d = 5.32\sqrt{t}$ $R^2 = 0.992$	-	-
10%	$C_d = 4.97\sqrt{t}$ $R^2 = 0.994$	6.62	0
20%	$C_d = 4.68\sqrt{t}$ $R^2 = 0.976$	11.91	0
25%	$C_d = 4.05\sqrt{t}$ $R^2 = 0.993$	23.88	0
30%	$C_d = 4.19\sqrt{t}$ $R^2 = 0.992$	21.27	0
40%	$C_d = 3.49\sqrt{t}$ $R^2 = 0.992$	33.32	0

(b) 20 ℃-curing

Fig. 8. Carbonation depth of GP mortars with different concentrations of AN application (Series No. 1, 9, 12, 13, 14, 15).

than that at the 7-day age, even for the 20 ℃-cured specimens. Dry shrinkage crack growth with age increased the internal diffusion of AN solution may be the reason for this experimental result. Additional experiments will be conducted to confirm this experimental phenomenon.

(2) Concentration of AN solution

Fig. 8 demonstrates the experimental results of the 70% FA/30% BFS blend-based GP mortars, which were modified on surfaces by different AN solutions with 10–40 wt% concentrations. And Fig. 9 shows the viscosity of each AN solution at 20 ℃, which was measured with a B-type viscometer. The viscosity of AN solution increases with its concentration, but from 30% to 40%, the viscosity sharply increases. In general, solutions with low viscosity have high permeability into GP materials [56].

Because the improvement in carbonation resistance of the AN treatment was small for the20 ℃-cured specimens, i.e. the decreasing rate of *a* value is low, the *a*-value decreasing rates obtained from the regression analysis were subject to relatively large experimental errors and therefore lacked a clear trend, as shown in the table of Fig.8 (b). But the ambient-cured GP has a loose microstructure at an early age, such as 3 days, compared to the heat-cured GP [57]. Thus, it is thought that even highly concentrated AN solutions have the potential to penetrate the inside of GP due to the loose structure. In fact, as shown in Fig. 8 (b), the greatest decrease in the *a*-value was observed when using the 40% AN solution.

However, from the experimental results of the 80℃-cured specimens, we found that when the concentration of AN solution was below 25%, the decreasing rate of *a* value was low, but when the concentration exceeded 25%, the decreasing rates of *a* value were very close for 25–40% concentration, but the *b* value showed a tendency to increase with increasing the AN concentration. This result can be explained by the following analysis: AN solution makes the surface layer of GP mortar dense through the generation of N-A-S-H gels and the filling effect after drying, thus delaying the onset of carbonation of GP. Therefore, although a highly concentrated AN solution does not tend to permeate much into the inside and increase the internal denseness, it greatly increases the denseness of the surface layer, resulting in an increase in the *b*-value. In contrast, a low concentration of AN solution cannot greatly increase the denseness of the surface layer due to the small amount of effective ingredients, but it can increase the denseness of the inside due to its high diffusion ability, thus reducing the carbonation rate coefficient *a*. However, if the concentration of AN solution is too small and thus its effective ingredients are few, even if it can diffuse to the inside of GP, the decrease of the carbonation rate coefficient *a* is limited.

Therefore, the 40% AN solution is recommended as a surface modifier for GP, regardless of whether the GP is cured at room temperature or high temperature. The surface treatment of 40% AN solution would reduce the carbonation rate coefficient of heat-cured GP mortar by about 70%, i.e. double the carbonation resistance. It also reduces the carbonation rate coefficient of ambient-cured GP mortar by more than 30% simultaneously. In combination with the AN surface treatment and the increase of GP compactness by optimising the use of raw materials and their proportions, it becomes easy to make the GP concrete reach the carbonation resistance of PC concrete of the same strength.

(3) Number of AN treatments and sealed curing after treatment

It is clearly shown in Fig. 10 that for the 20 ℃-cured GP mortars, as the number of AN surface treatments at 3-day age increased from once to twice, the carbonation rate coefficient *a* decreased, but the delaying of carbonation was not found (*b* value was zero). However, for the 80 ℃-cured GP mortars, increasing the number of AN treatments had almost no effect on the carbonation rate coefficient *a*, but the beginning of carbonation was delayed (*b* value increased), which indicates that the 2 treatments increased the denseness of the GP surface layer more than the one treatment.

For the 80 ℃-cured specimens, the drying of specimens and the occurrence of drying shrinkage cracks make the penetration of AN solution easier, so a single treatment can largely reduce the *a* value, but the rapid internal penetration of AN solution with less surface stay requires twice treatment. However, for the specimens cured at 20 ℃, high moisture content and few cracks make the penetration of AN solution not easy. Thus, several times treatment is needed. Even several times in treatment, it is difficult to make the surface layer dense due to the presence of moisture in the surface layer during treatment. Although the twice treatment delayed the onset of carbonation, they did not change the carbonation rate coefficient of the 80 ℃-cured specimens. Therefore, from the perspective of long-term carbonation depth, once treatment is also an option for GPs cured at high temperatures.

Fig. 11 demonstrates the influence of sealed curing after the AN surface treatment on the *a*, *b* values. The sealing did not further contribute to much improvement in the carbonation resistance of the 80 ℃-cured specimens, but the beginning of carbonation was delayed for two weeks. This means that the specimens without sealing were carbonated during the curing period. However, the sealing decreased the carbonation rate coefficient of the 20 ℃-cured specimens, but the beginning of carbonation was not yet delayed. Therefore, from the perspective of long-term carbonation depth, unsealed curing after the AN treatment is an option for simplifying construction if GPs are cured at

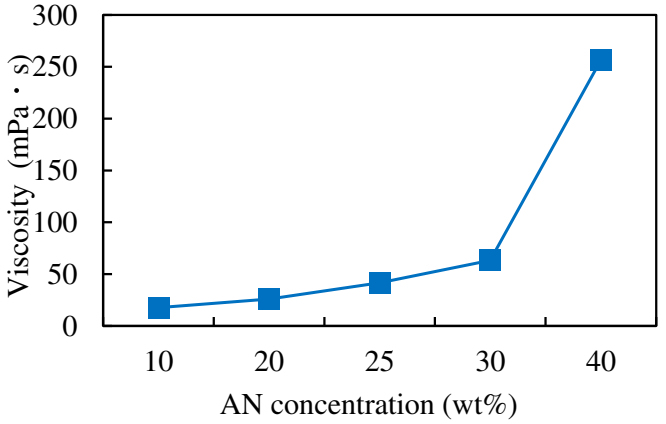

Fig. 9. Viscosities of AN solutions with different concentrations.

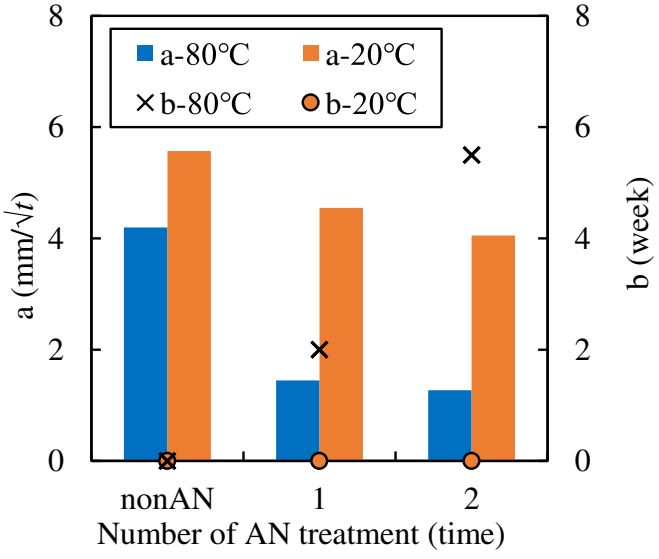

Fig. 10. The changes of the *a*, *b*-values with number of AN treatment.

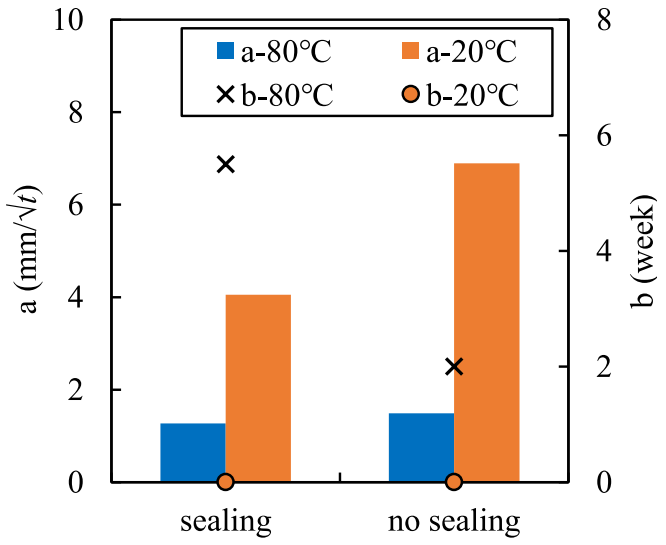

Fig. 11. Influences of sealed curing on the *a*, *b*-values.

high temperatures, but for the ambient-cured GPs, sealed curing is recommended.

3.3. Air permeability and strength of surface-modified GP mortars

Fig. 12 illustrates the air permeability of the GP mortar specimens cured by the 20 ℃-curing method or the 80 ℃-curing method. It shows that no matter what curing method was used, the AN surface treatment greatly reduced the air permeability of the GP mortar specimens, which suggests that the internal structure of GP can become dense if the GP surface is modified by the AN solution. As described later, the AN treatment at least decreased the cracks in the surface layer of GP mortar.

We found that the air permeability of 80 ℃-cured GP mortar specimens had higher air permeability compared with the 20 ℃-cured specimens. This result was consistent with the results reported by other studies [58,59]. However, as shown in Figs. 3-9, the 80 ℃-cured specimens had smaller carbonation rate coefficients *a* than the 20 ℃-cured specimens. This can be explained by the following reasons. Due to dry shrinkage, the geopolymer experienced the 80 ℃-curing has large cracks with sizes of 0.01–0.1 μm, while the geopolymer cured only at 20 ℃ has more capillary cracks whose sizes are mostly below 0.01 μm [60]. Large cracks result in higher air permeability. However, it is no doubt that heat-curing contributes to many formations of geopolymeric products and, thus a dense microstructure [40,41], which makes CO_2 diffusion difficult into the geopolymeric matrix between large cracks. Therefore, although the 80 ℃-cured GP mortar specimens had higher air permeability, but their carbonation rate coefficients were smaller compared with the 20 ℃-cured specimens.

Fig.13 shows the flexural and compressive strengths of series No.1 and No.3. We found that the AN surface treatment did not almost affect the strengths of BFS/FA blend-based GP mortar, regardless of the curing method used. This is because the diffusion of the AN solution only reached the surface layer of the GP mortars.

3.4. SEM-EDS results of surface-modified GP mortar

In the SEM analysis, in addition to the structural changes observed by SEM images, elemental analysis (EDS) was also performed to determine the changes in gel compositions. Since gel microstructure is significantly related to the SiO_2/Al_2O_3 ratio [61], we calculated the average mole ratio of SiO_2/Al_2O_3 for the whole analysed area.

(1) FA-based GP mortar

Fig.14 (a) and (b) show the SEM results of FA-based GP mortar (series No. 2) with and without AN surface treatment after the accelerated carbonation test of 12 weeks. First, the AN surface-treated mortar was found to be denser than the mortar without the AN treatment, although the pores remained. In the former, almost no cracks are observed. The reduction in cracks may be due to the AN treatment, which reduced the drying shrinkage cracks caused by water evaporation. Although the AN-treated mortar became relatively dense, it still has a low resistance to carbonation because of the large number of tiny pores.

Fly ash particles with smooth surfaces can be found to remain in the two mortars. However, many fly ash particles in the AN-treated mortar were surrounded by dense gels or were corroded, which suggests that reaction products increased. During the accelerated carbonation test, the CO_2 reacted with the Na^+ remaining in the pores to form Na_2CO_3 [62]. Since Na^+ is used to balance the Al^{3+} charge of the $Al(OH)_4$ tetrahedra, an increase in N-A-S-H gels would reduce the residual Na^+ in the pores. Hence, we found there are many needle crystals in the FA-

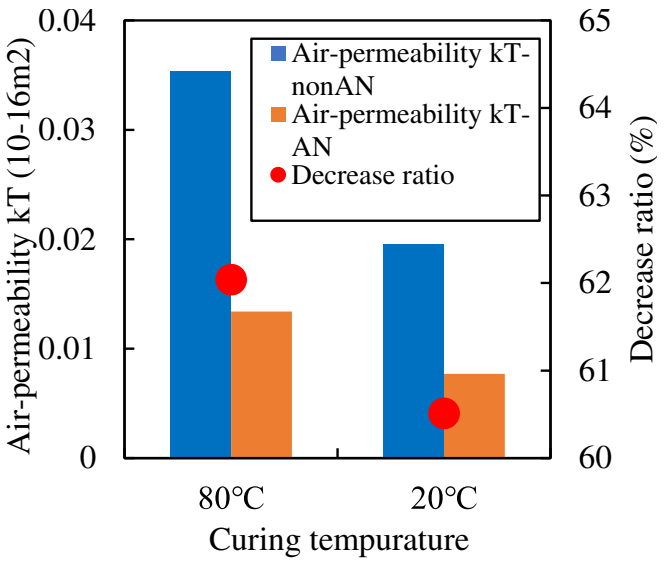

Fig. 12. Air-permeability of GP mortars with and without AN surface treatment.

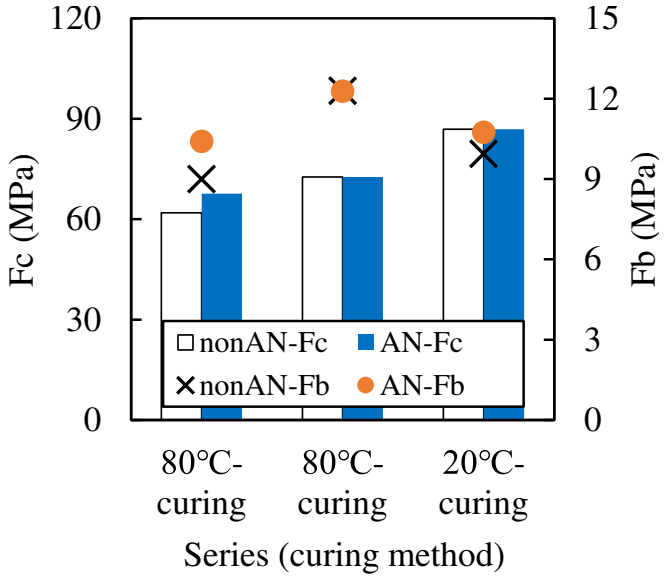

Fig. 13. Comparison of strengths of GP mortars with and without AN surface treatment.

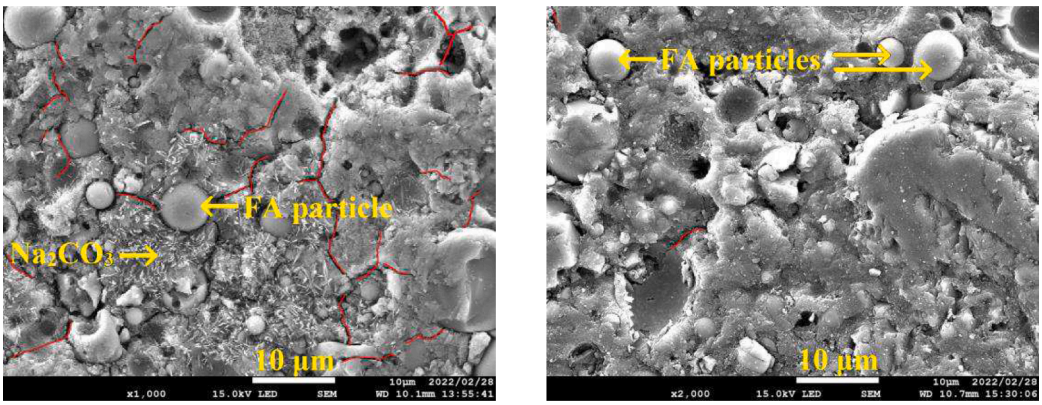

(a) Non-AN treatment (b) AN treatment

Fig. 14. SEM images of FA-based GP mortars.

based GP mortar without the AN treatment, while needle crystals are rarely found in the mortar after AN surface treatment.

The microstructure of geopolymer is strongly influenced by the SiO_2/Al_2O_3 ratio, and geopolymer with a lower SiO_2/Al_2O_3 has a dense structure [59,63–66]. As shown in Table 6, the SiO_2/Al_2O_3 ratio of FA-based GP mortar decreased with the AN treatment. Thus, the AN-treated mortar has a denser microstructure than the mortar without the AN treatment, which also means higher carbonation resistance of GP materials.

(2) BFS-based GP mortar

Fig.15 shows the SEM images for the BFS-based GP mortars (series No. 4) without and with the AN treatment. The BFS-based GP mortars without the AN treatment had relatively dense microstructure. However, the AN treatment obviously reduced tiny cracks, resulting in a denser GP mortar. As stated above, the AN treatment decreases the cracks caused by dry shrinkage. In the GP mortar without the AN treatment, many $CaCO_3$ crystals are found (see Fig. 15 (a)), while in the AN-treated mortar, $CaCO_3$ crystals are very few (see Fig. 15 (b)). The products of BFS-based GP are main C-A-S-H gels [67–69]. As the carbonation reaction proceeds, the C-A-S-H gel undergoes decalcification, and various calcium carbonate polymorphs are formed [70]. However, the AN treatment may strengthen the structure of the C-A-S-H gel due to the Al^{3+} provided by the AN solution, making the C-A-S-H gel less susceptible to decalcification.

Duxson [63] reported that the denseness of geopolymer increases with the decrease in SiO_2/Al_2O_3 ratio. The abundant Al_2O_3 provided by AN decreased the SiO_2/Al_2O_3 ratio, as shown in Table 7, contributing to the denser microstructure of AN-treated GP mortar and improved carbonation resistance, which was also reflected in the reduction of $CaCO_3$. The above factors, including the reduction in cracks and strengthened C-A-S-H gel structure, collectively contributed to the carbonation resistance improvement of BFS-based GP mortars with AN treatment.

(3) FA/BFS blend-based GP mortar

Table 6
Comparison of average mole ratios of oxids of FA-based GP mortars with and without AN treatment.

AN treatment	Na (%)	Mg (%)	Al (%)	Si (%)	Ca (%)	SiO_2/Al_2O_3	SiO_2/CaO
Non	6.23	0.60	5.19	14.15	1.76	5.45	8.04
Treated	3.67	0.44	6.35	12.40	1.22	3.90	10.16

Fig. 16 shows the SEM images of FA/BFS blend-based GP mortars (series No. 1) with and without AN surface treatment. Calcite is observed in the two mortars, but in the mortar with AN treatment, the calcite crystals are few, suggesting the reaction of CO_2 and Ca^{2+} that originated from decalcification of C-A-S-H gels was deceased because of AN treatment. Also, the mortar with the AN surface treatment had few fine cracks, compared to the mortar without the AN treatment. As explained before, AN treatment would reduce the cracks caused by dry shrinkage. Because the polycondensation of geopolymer is a dehydration reaction, consuming no water [12], large dry shrinkage may be resulted in a dense surface layer formed by AN surface treatment, reducing the escape of inside moisture, which contributed to the decrease of drying shrinkage cracks. Hence, the air permeability coefficient of AN-treated mortar was reduced, as shown in Fig. 12, and because of the decrease in drying shrinkage cracks, the carbonation was slowed down. Combining the decrease of the SiO_2/Al_2O_3 ratio (see Table 8), we can conclude that the AN treatment increases the denseness of geopolymer and reduces the dry shrinkage and decalcification of geopolymer.

3.5. XRD results of surface-modified GP mortar

Fig. 17 shows the XRD patterns for three types of GP mortars, which used the same alkali activator solutions and the same fine aggregate, but different precursor(s), and for the raw materials that were BFS, FA and sea sand. Raw BFS has almost no crystal, and fly ash has only quartz and mullite. The sea sand, washed with tap water, contains quartz, mullite, gismondine, and Na-gmelinite. The three GP mortars had almost the same crystal phases with their raw materials. That is to say, the AN treatment did not generate any new crystalline product. But for the BFS-based GP mortar, the AN treatment increased the intensity of gismondine. Plenty of Ca and Al promoted the formation of gismondine [71]. Obvious calcite was detected in the BFS-based GP specimens, which corresponded to the results of SEM results. For the FA-based and FA/BFS blend-based GP mortars, the difference between the XRD patterns of the specimens with and without the AN treatment was the peak intensity of Na-gmelinite. Although Na-gmelinite is also present in the sand [72], the peak intensity of Na-gmelinite was dramatically increased due to the AN treatment. Bae, et al. [73] also reported that adding a high amount of $NaAlO_2$ in geopolymer would form Na-gmelinite. In the FA-based GP mortars, the peaks of Na_2CO_3 were detected, which corresponded to the observation of Na_2CO_3 in the SEM images. The increase of Na-gmelinite and gismondine caused by the AN treatment reduced the pores of the geopolymer matrix and thus inhibited the permeation of carbon dioxide.

4. Conclusions and future works

In this study, to address the problem of low carbonation

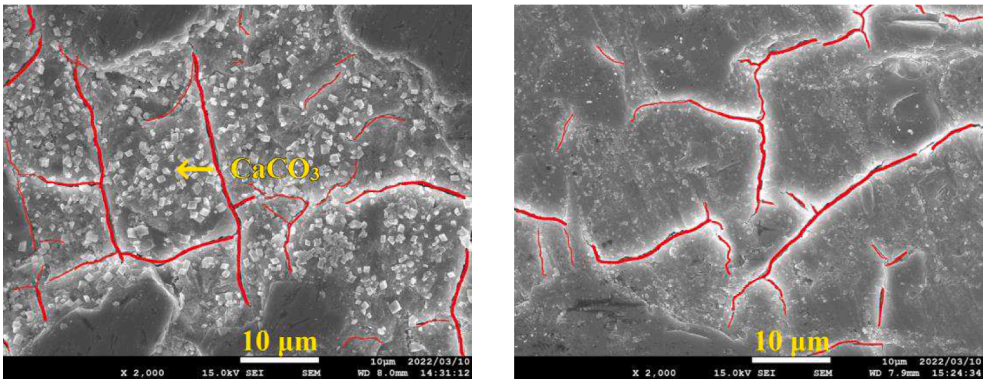

(a) Non-AN application (b) AN application

Fig. 15. SEM images of BFS-based GP mortars.

Table 7
Comparison of average mole ratios of oxids of BFS-based GP mortars with and without AN treatment.

AN treatment	Na (%)	Mg (%)	Al (%)	Si (%)	Ca (%)	SiO_2/Al_2O_3	SiO_2/CaO
Non-AN	6.49	1.53	2.78	7.87	8.57	5.66	0.91
AN	2.80	1.83	4.46	10.67	9.77	4.78	1.09

(neutralization) resistance of geopolymer (GP), which is very difficult to be solved by mixture design alone, we investigated the effect of sodium aluminate aqueous solution (AN) used as inorganic surface modifier, which is expected to be more durable than organic surface coating, on the carbonation resistance of geopolymers. The carbonation depths of different GP mortars were measured to clarify the effects of mixture and curing method on the benefits of using AN. We also discussed suitable AN application conditions and the mechanisms by which AN surface modification improves the carbonation resistance of GP. The conclusions obtained are summarized as follows.

The surface modification of AN significantly reduced the carbonation rate coefficient of GP mortars regardless of curing temperature of mortar, and largely delayed the onset of neutralization of heat-cured GP mortars. The heat-cured geopolymers can benefit more from the AN surface modification than the ambient-cured geopolymers in the carbonation resistance improvement.

The AN surface modification improved the carbonation resistance of FA/BFS blend-based geopolymers more significantly, particularly when the blending ratio of FA was higher, compared to the geopolymers using BFS or FA alone as precursor. The carbonation rate coefficients of FA/BFS blend-based GPs with the heat-curing and the ambient curing can be reduced by about 70% and more than 30%, respectively. The AN surface modification even made the carbonation depth of the FA/BFS blend-based, heat-cured GP mortar undetectable within the accelerated carbonation test period (18 weeks, see Fig.4(a)).

The smaller the liquid-active filler ratio (AS/AF), the larger the improvement in carbonation resistance caused by the AN surface modification. However, the influence of the compositions of alkali activator on the effectiveness of AN surface modification is uncertain due to the complex factors such as the alkalinity of residual alkali activator, the reactivity of alkali activator and AN, the denseness of GP that is affected by the compositions of alkali activator.

The AN surface modification reduced surface cracks and improved the denseness of surface layer of GP due to the formation of Na-gmelinite and gismondine in addition to the reduction of dry shrinkage, which reduced CO_2 permeability but did not increase the strength of GP.

The optimal conditions for AN surface treatment were found to be 40% concentration by mass at 3-day age, with twice surface treatment preferred for ambient-cured geopolymer and once for heat-

Table 8
Comparison of average mole ratios of oxides of BFS/FA blend-based GP mortars with and without AN treatment.

AN application	Na (%)	Mg (%)	Al (%)	Si (%)	Ca (%)	SiO_2/Al_2O_3	SiO_2/CaO
Non-AN	2.30	0.84	3.92	13.16	4.68	6.71	2.81
AN	2.75	1.16	3.75	11.07	5.59	5.90	1.98

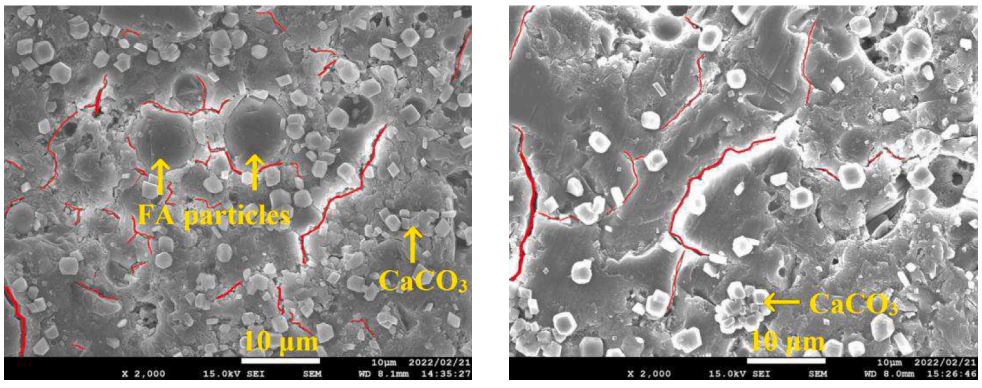

(a) Non-AN application (b) AN application

Fig. 16. SEM images of FA/BFS blend-based GP mortars.

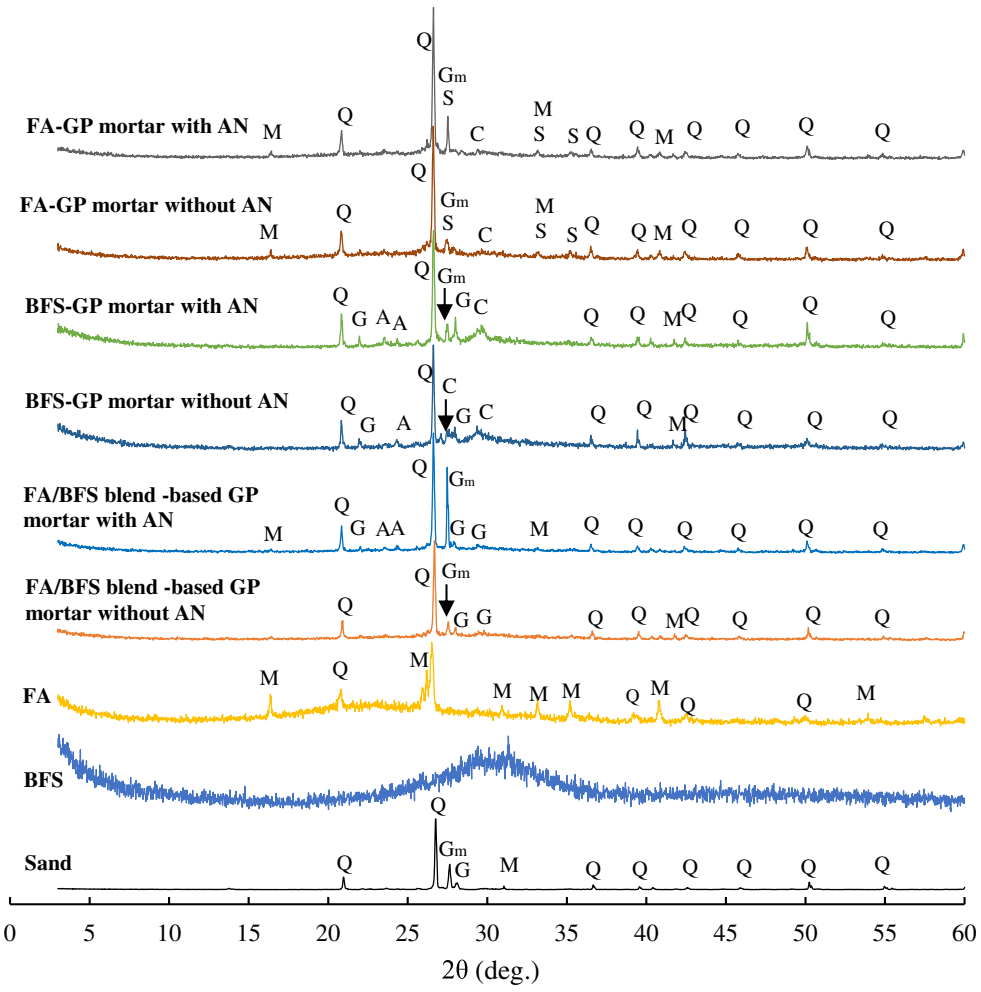

Fig. 17. XRD pattern of specimens for FA, BFS, FA/BFS-based GP mortars. [Notes] Q: Quartz, M: Mullite, A: Albite, C: Calcite, G: Gismondine, G_m: Na-gmelinite, S: Sodium carbonate.

cured geopolymer. And after the surface treatment, it is best to seal the GP during its continued curing period.

The AN surface treatment method used in this study did not provide a very high improvement in the carbonation resistance for ambient-cured GP. Further investigation on treatment method and additive of AN surface modifier will be conducted. Moreover, from the point of view of waste utilization, the research on geopolymers using BFS/FA as precursors has been increasing significantly recently. Therefore, the present study discussed, as a prioritized step, the effectiveness of AN surface modification for the geopolymers with BFS, FA as precursor(s). However, from the improvement mechanisms explained in Sections 3.4 and 3.5, it is highly likely that this approach is also applicable to the geopolymers using other kinds of precursor such as metakaolin and a blend of BFS and other fillers except FA, and can improve other properties of geopolymers such as frost resistance and chloride permeability. Thus, we will continue to investigate the effects of using this surface modification technique on the durability of various geopolymers in the future. This study will contribute to the establishment of effective techniques to ensure the durability of GP for forwarding the practical application of GP in reinforced concrete.

CRediT authorship contribution statement

Xuezhong LI: Validation, Investigation, Writing – original draft, Visualization, Data curation. **Zhuguo LI:** Conceptualization, Methodology, Validation, Writing – review & editing, Funding acquisition, Supervision, Project administration.

Declaration of Competing Interest

The authors declare that they have no known competing financial interests or personal relationships that could have appeared to influence the work reported in this paper.

Data availability

No data was used for the research described in the article.

References

[1] A. Mehta, R. Siddique, An overview of geopolymers derived from industrial by-products, Constr. Build. Mater. 127 (2016) 183–198, https://doi.org/10.1016/j.conbuildmat.2016.09.136.
[2] L.K. Turner, F.G. Collins, Carbon dioxide equivalent (CO2-e) emissions: A comparison between geopolymer and OPC cement concrete, Constr. Build. Mater. 43 (2013) 125–130, https://doi.org/10.1016/j.conbuildmat.2013.01.023.
[3] D.N. Huntzinger, T.D. Eatmon, A life-cycle assessment of Portland cement manufacturing: comparing the traditional process with alternative technologies, J. Clean. Prod. 17 (7) (2009) 668–675.
[4] P. Duxson, A. Fernández-Jiménez, J.L. Provis, G.C. Lukey, A. Palomo, J.S.J. van Deventer, Geopolymer technology: the current state of the art, J. Mater. Sci. 42 (9) (2007) 2917–2933.
[5] C. Li, H. Sun, L. Li, A review: the comparison between alkali-activated slag (Si+ Ca) and metakaolin (Si+ Al) cements, Cem. Concr. Res. 40 (9) (2010) 1341–1349.

[6] J. Davidovits, L. Buzzi, P. Rocher, D. Gimeno, C. Marini, S. Tocco, Geopolymeric cement based on low cost geologic materials. Results from the european research project geocistem, in: Proc. 2nd Int. Conf. Geopolymer, (1999) 83–96.
[7] J. Davidovits, Geopolymers: inorganic polymeric new materials, J. Therm. Anal. Calorim. 37 (8) (1991) 1633–1656.
[8] K.A. Komnitsas, Potential of geopolymer technology towards green buildings and sustainable cities, Procedia Eng. 21 (2011) 1023–1032.
[9] J. Zeng, Y. Zhuge, S. Liang, Y. Bai, J. Liao, L. Zhang, Durability assessment of PEN/PET FRP composites based on accelerated aging in alkaline solution/seawater with different temperatures, Constr. Build. Mater. 327 (2022), 126992, https://doi.org/10.1016/j.conbuildmat.2022.126992.
[10] J. Zeng, D. Zhu, J. Liao, Y. Zhuge, Y. Bai, L. Zhang, Large-rupture-strain (LRS) FRP-confined concrete in square stub columns: Effects of specimen size and assessments of existing models, Constr. Build. Mater. 326 (2022), 126869, https://doi.org/10.1016/j.conbuildmat.2022.126869.
[11] J. Zeng, J. Liao, Y. Zhuge, Y. Guo, J. Zhou, Z. Huang, L. Zhang, Bond behavior between GFRP bars and seawater sea-sand fiber-reinforced ultra-high strength concrete, Eng. Struct. 254 (2022), 113787, https://doi.org/10.1016/j.engstruct.2021.113787.
[12] H. Xu, J.S.J. Van Deventer, The geopolymerisation of alumino-silicate minerals, Int. J. Miner. Process. 59 (3) (2000) 247–266.
[13] Z. Li, Z. Ding, Y. Zhang, Development of sustainable cementitious materials, in: Proc. Int. Work. Sustain. Dev. Concr. Technol. Beijing, China, (2004) 55–76.
[14] G. Kürklü, The effect of high temperature on the design of blast furnace slag and coarse fly ash-based geopolymer mortar, Compos. B Eng. 92 (2016) 9–18.
[15] G.A. Khoury, Compressive strength of concrete at high temperatures: a reassessment, Mag. Concr. Res. 44 (161) (1992) 291–309.
[16] V. Vydra, F. Vodák, O. Kapičková, Š. Hošková, Effect of temperature on porosity of concrete for nuclear-safety structures, Cem. Concr. Res. 31 (7) (2001) 1023–1026.
[17] X. Fu, Q. Li, J. Zhai, G. Sheng, F. Li, The physical–chemical characterization of mechanically-treated CFBC fly ash, Cem. Concr. Compos. 30 (3) (2008) 220–226.
[18] J.G.S. van Jaarsveld, J.S.J. van Deventer, Effect of the alkali metal activator on the properties of fly ash-based geopolymers, Ind. Eng. Chem. Res. 38 (10) (1999) 3932–3941.
[19] R. Kumar, S. Kumar, S.P. Mehrotra, Towards sustainable solutions for fly ash through mechanical activation, Resour. Conserv. Recycl. 52 (2) (2007) 157–179.
[20] H. Xu, J.S.J. Van Deventer, Geopolymerisation of multiple minerals, Miner. Eng. 15 (12) (2002) 1131–1139.
[21] B. Zhang, K.J.D. MacKenzie, I.W.M. Brown, Crystalline phase formation in metakaolinite geopolymers activated with NaOH and sodium silicate, J. Mater. Sci. 44 (17) (2009) 4668–4676.
[22] B. Pandey, S.D. Kinrade, L.J.J. Catalan, Effects of carbonation on the leachability and compressive strength of cement-solidified and geopolymer-solidified synthetic metal wastes, J. Environ. Manage. 101 (2012) 59–67, https://doi.org/10.1016/j.jenvman.2012.01.029.
[23] S.A. Bernal, J.L. Provis, D.G. Brice, A. Kilcullen, P. Duxson, J.S.J. van Deventer, Accelerated carbonation testing of alkali-activated binders significantly underestimates service life: The role of pore solution chemistry, Cem. Concr. Res. 42 (10) (2012) 1317–1326.
[24] Z. Li, S. Li, Carbonation resistance of fly ash and blast furnace slag based geopolymer concrete, Constr. Build. Mater. 163 (2018) 668–680.
[25] K. Pasupathy, M. Berndt, A. Castel, J. Sanjayan, R. Pathmanathan, Carbonation of a blended slag-fly ash geopolymer concrete in field conditions after 8 years, Constr. Build. Mater. 125 (2016) 661–669.
[26] R. Pouhet, M. Cyr, Carbonation in the pore solution of metakaolin-based geopolymer, Cem. Concr. Res. 88 (2016) 227–235, https://doi.org/10.1016/j.cemconres.2016.05.008.
[27] S. Li, Z. Li, T. Nagai, T. Okata, Neutralization resistance of fly ash and blast furnace slag based geopolymer concrete, Proc. Jpn. Concr. Inst. 39 (1) (2017) 2023–2028.
[28] R.A. Robayo-Salazar, A.M. Aguirre-Guerrero, R. Mejía de Gutiérrez, Carbonation-induced corrosion of alkali-activated binary concrete based on natural volcanic pozzolan, Constr. Build. Mater. 232 (2020), 117189, https://doi.org/10.1016/j.conbuildmat.2019.117189.
[29] V. Charitha, G. Athira, A. Bahurudeen, S. Shekhar, Carbonation of alkali activated binders and comparison with the performance of ordinary Portland cement and blended cement binders, J. Build. Eng. 53 (2022), 104513, https://doi.org/10.1016/j.jobe.2022.104513.
[30] J.S.J. Van Deventer, J.L. Provis, P. Duxson, Technical and commercial progress in the adoption of geopolymer cement, Miner. Eng. 29 (2012) 89–104.
[31] P. Duxson, J.L. Provis, G.C. Lukey, J.S.J. Van Deventer, The role of inorganic polymer technology in the development of 'green concrete', Cem. Concr. Res. 37 (12) (2007) 1590–1597.
[32] T. Xie, T. Ozbakkaloglu, Behavior of low-calcium fly and bottom ash-based geopolymer concrete cured at ambient temperature, Ceram. Int. 41 (4) (2015) 5945–5958, https://doi.org/10.1016/j.ceramint.2015.01.031.
[33] Z. Li, S. Li, Effects of wetting and drying on alkalinity and strength of fly ash/slag-activated materials, Constr. Build. Mater. 254 (2020) 119, https://doi.org/10.1016/j.conbuildmat.2020.119069.
[34] S.A. Bernal, R. San Nicolas, R.J. Myers, R.M. de Gutiérrez, F. Puertas, J.S.J. van Deventer, J.L. Provis, MgO content of slag controls phase evolution and structural changes induced by accelerated carbonation in alkali-activated binders, Cem. Concr. Res. 57 (2014) 33–43.
[35] M. Zhang, H. Xu, A.L. Phalé Zeze, X. Liu, M. Tao, Coating performance, durability and anti-corrosion mechanism of organic modified geopolymer composite for marine concrete protection, Cem. Concr. Compos. 129 (2022), 104495, https://doi.org/10.1016/j.cemconcomp.2022.104495.
[36] S. Kitasato, Z. Li, Experimental study on the properties of geopolymer concrete using fly ash and ground granulated blast furnace slag, part 14: effects of coating agent, Summ. Tech. Pap. Annu. Meet. AIJ. 2017 (2017) 751–752.
[37] W. Yu, Z. Wenhua, W. Peipei, P. Yilin, Z. Yunsheng, Study on preparation and strengthening mechanism of new surface treatment agent of concrete at multi-scale, Constr. Build. Mater. 346 (2022), 128404, https://doi.org/10.1016/j.conbuildmat.2022.128404.
[38] L. Jiang, X. Xue, W. Zhang, J. Yang, H. Zhang, Y. Li, R. Zhang, Z. Zhang, L. Xu, J. Qu, J. Song, J. Qin, The investigation of factors affecting the water impermeability of inorganic sodium silicate-based concrete sealers, Constr. Build. Mater. 93 (2015) 729–736, https://doi.org/10.1016/j.conbuildmat.2015.06.001.
[39] P.C. Tran, K. Kobayashi, T. Asano, S. Kojima, Carbonation proofing mechanism of silicate-based surface impregnations, J. Adv. Concr. Technol. 16 (10) (2018) 512–521.
[40] S. Muthukrishnan, S. Ramakrishnan, J. Sanjayan, Effect of microwave heating on interlayer bonding and buildability of geopolymer 3D concrete printing, Constr. Build. Mater. 265 (2020), 120786, https://doi.org/10.1016/j.conbuildmat.2020.120786.
[41] M. Lahoti, S.F. Wijaya, K.H. Tan, E.-H. Yang, Tailoring sodium-based fly ash geopolymers with variegated thermal performance, Cem. Concr. Compos. 107 (2020), 103507, https://doi.org/10.1016/j.cemconcomp.2019.103507.
[42] J. Ye, W. Zhang, D. Shi, Effect of elevated temperature on the properties of geopolymer synthesized from calcined ore-dressing tailing of bauxite and ground-granulated blast furnace slag, Constr. Build. Mater. 69 (2014) 41–48, https://doi.org/10.1016/j.conbuildmat.2014.07.002.
[43] J. Shi, B. Liu, S. Chu, Y. Zhang, Z. Di Zhang, K.D. Han, Recycling air-cooled blast furnace slag in fiber reinforced alkali-activated mortar, Powder Technol. 407 (2022), 117686, https://doi.org/10.1016/j.powtec.2022.117686.
[44] C. Gunasekara, D.W. Law, S. Setunge, Long term permeation properties of different fly ash geopolymer concretes, Constr. Build. Mater. 124 (2016) 352–362, https://doi.org/10.1016/j.conbuildmat.2016.07.121.
[45] S.A. Bernal, R. Mejía de Gutiérrez, J.L. Provis, Engineering and durability properties of concretes based on alkali-activated granulated blast furnace slag/metakaolin blends, Constr. Build. Mater. 33 (2012) 99–108, https://doi.org/10.1016/j.conbuildmat.2012.01.017.
[46] Y. Luna Galiano, C. Fernández Pereira, M. Izquierdo, Contributions to the study of porosity in fly ash-based geopolymers. Relationship between degree of reaction, porosity and compressive strength, Mater. Construcción. 66 (324) (2016), https://doi.org/10.3989/mc.2016.10215.
[47] J.L. Provis, R.J. Myers, C.E. White, V. Rose, J.S.J. Van Deventer, X-ray microtomography shows pore structure and tortuosity in alkali-activated binders, Cem. Concr. Res. 42 (6) (2012) 855–864.
[48] H. Cheng, K.-L. Lin, R. Cui, C.-L. Hwang, Y.-M. Chang, T.-W. Cheng, The effects of SiO2/Na2O molar ratio on the characteristics of alkali-activated waste catalyst–metakaolin based geopolymers, Constr. Build. Mater. 95 (2015) 710–720, https://doi.org/10.1016/j.conbuildmat.2015.07.028.
[49] K. Ghosh, P. Ghosh, Effect of% Na2O and% SiO2 on apperent porosity and sorptivity of fly ash based geopolymer, IOSR J. Eng. 2 (2012) 96–101.
[50] R. Pouhet, M. Cyr, R. Bucher, Influence of the initial water content in flash calcined metakaolin-based geopolymer, Constr. Build. Mater. 201 (2019) 421–429, https://doi.org/10.1016/j.conbuildmat.2018.12.201.
[51] C.E. White, J.L. Provis, T. Proffen, J.S.J. Van Deventer, The effects of temperature on the local structure of metakaolin-based geopolymer binder: A neutron pair distribution function investigation, J. Am. Ceram. Soc. 93 (10) (2010) 3486–3492.
[52] L. Tian, D. He, J. Zhao, H. Wang, Durability of geopolymers and geopolymer concretes: A review, Rev. Adv. Mater. Sci. 60 (1) (2021) 1–14.
[53] Z. Zhang, H. Wang, J.L. Provis, A. Reid, Efflorescence: a critical challenge for geopolymer applications?, in: Concr. Inst. Aust. Bienn. Natl. Conf. 2013, Concrete Institute of Australia, (2013) 1–10.
[54] O.A. Abdulkareem, M. Ramli, J.C. Matthews, Production of geopolymer mortar system containing high calcium biomass wood ash as a partial substitution to fly ash: An early age evaluation, Compos. B Eng. 174 (2019), 106941, https://doi.org/10.1016/j.compositesb.2019.106941.
[55] M.T. Marvila, A.R.G. Azevedo, G.C.G. Delaqua, B.C. Mendes, L.G. Pedroti, C.M. F. Vieira, Performance of geopolymer tiles in high temperature and saturation conditions, Constr. Build. Mater. 286 (2021), 122994, https://doi.org/10.1016/j.conbuildmat.2021.122994.
[56] Y. Wang, J. Zhao, J. Chen, Effect of polydimethylsiloxane viscosity on silica fume-based geopolymer hybrid coating for flame-retarding plywood, Constr. Build. Mater. 239 (2020), 117814, https://doi.org/10.1016/j.conbuildmat.2019.117814.
[57] T. Suwan, M. Fan, Influence of OPC replacement and manufacturing procedures on the properties of self-cured geopolymer, Constr. Build. Mater. 73 (2014) 551–561, https://doi.org/10.1016/j.conbuildmat.2014.09.065.
[58] F.G.M. Aredes, T.M.B. Campos, J.P.B. Machado, K.K. Sakane, G.P. Thim, D. D. Brunelli, Effect of cure temperature on the formation of metakaolinite-based geopolymer, Ceram. Int. 41 (6) (2015) 7302–7311, https://doi.org/10.1016/j.ceramint.2015.02.022.
[59] Z. Kubba, G. Fahim Huseien, A.R.M. Sam, K.W. Shah, M.A. Asaad, M. Ismail, M. M. Tahir, J. Mirza, Impact of curing temperatures and alkaline activators on compressive strength and porosity of ternary blended geopolymer mortars, Case Stud, Constr. Mater. 9 (2018) e00205.
[60] P. Rovnaník, Effect of curing temperature on the development of hard structure of metakaolin-based geopolymer, Constr. Build. Mater. 24 (7) (2010) 1176–1183, https://doi.org/10.1016/j.conbuildmat.2009.12.023.

[61] P. De Silva, K. Sagoe-Crenstil, V. Sirivivatnanon, Kinetics of geopolymerization: Role of Al2O3 and SiO2, Cem. Concr. Res. 37 (4) (2007) 512–518, https://doi.org/10.1016/j.cemconres.2007.01.003.
[62] N. Sedira, J. Castro-Gomes, Microstructure Features of Ternary Alkali-activated Binder Based on Tungsten Mining Waste, Slag and Metakaolin, KnE Eng. 5 (4 SE-Articles) (2020), https://doi.org/10.18502/keg.v5i4.6810.
[63] P. Duxson, J.L. Provis, G.C. Lukey, S.W. Mallicoat, W.M. Kriven, J.S.J. Van Deventer, Understanding the relationship between geopolymer composition, microstructure and mechanical properties, Colloids Surfaces A Physicochem. Eng. Asp. 269 (1–3) (2005) 47–58.
[64] M. Steveson, K. Sagoe-Crentsil, Relationships between composition, structure and strength of inorganic polymers, J. Mater. Sci. 40 (8) (2005) 2023–2036, https://doi.org/10.1007/s10853-005-1226-2.
[65] M. Rowles, B. O'connor, Chemical optimisation of the compressive strength of aluminosilicate geopolymers synthesised by sodium silicate activation of metakaolinite, J. Mater. Chem. 13 (5) (2003) 1161–1165.
[66] R.A. Fletcher, K.J.D. MacKenzie, C.L. Nicholson, S. Shimada, The composition range of aluminosilicate geopolymers, Journal of the European Ceramic Society 25 (9) (2005) 1471–1477, https://doi.org/10.1016/j.jeurceramsoc.2004.06.001.
[67] Z. Li, R. Kondo, K. Ikeda, Recycling of waste Incineration bottom ash and heavy metal immobilization by geopolymer production, J. Adv. Concr. Technol. 19 (4) (2021) 259–279, https://doi.org/10.3151/jact.19.259.
[68] A. D'Elia, D. Pinto, G. Eramo, R. Laviano, A. Palomo, A. Fernández-Jiménez, Effect of Alkali Concentration on the Activation of Carbonate-High Illite Clay, Appl. Sci. 10 (7) (2020), https://doi.org/10.3390/app10072203.
[69] S. Zhao, M. Xia, L. Yu, X. Huang, B. Jiao, D. Li, Optimization for the preparation of composite geopolymer using response surface methodology and its application in lead-zinc tailings solidification, Constr. Build. Mater. 266 (2021), 120969, https://doi.org/10.1016/j.conbuildmat.2020.120969.
[70] A.E. Morandeau, C.E. White, In situ X-ray pair distribution function analysis of accelerated carbonation of a synthetic calcium–silicate–hydrate gel, J. Mater. Chem. A 3 (16) (2015) 8597–8605.
[71] J.E. Oh, J. Moon, S.-G. Oh, S.M. Clark, P.J.M. Monteiro, Microstructural and compositional change of NaOH-activated high calcium fly ash by incorporating Na-aluminate and co-existence of geopolymeric gel and C-S–H(I), Cem. Concr. Res. 42 (5) (2012) 673–685, https://doi.org/10.1016/j.cemconres.2012.02.002.
[72] W.S. Wise, The Na-rich zeolites from Boron, California, in: A. Gamba, C. Colella, S. B.T.-S. in S.S. and C. Coluccia (Eds.), Oxide Based Mater., Elsevier, (2005) 13–18.
[73] S.J. Bae, S. Park, H.K. Lee, Role of Al in the crystal growth of alkali-activated fly ash and slag under a hydrothermal condition, Constr. Build. Mater. 239 (2020), 117842, https://doi.org/10.1016/j.conbuildmat.2019.117842.